Electrocatalysis in confinement: metal-organic frameworks for oxygen reduction

Hoefnagel, M.E.

Appendix A

Supplementary information for Chapter 2:

Directing the Selectivity of Oxygen Reduction to Water by Confining a Cu catalyst in a Metal-Organic Framework

A1 Powder X-ray Diffraction

PXRD patterns before catalysis (Figure A1, black line) and after catalysis (Figure A1, grey line) were measured for NU1000|Cu-tmpaCOOH drop casted onto an FTO electrode with carbon black to characterize structural integrity of the MOF.

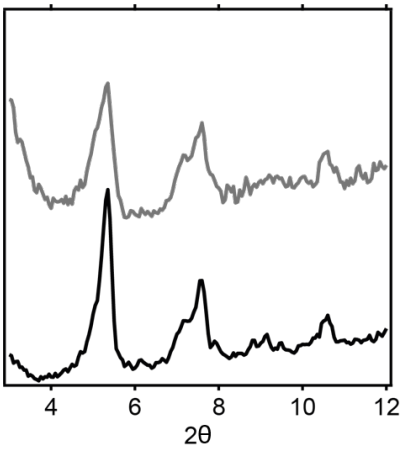

Figure A1. PXRD patterns of NU1000|Cu-tmpaCOOH dropcasted on FTO with carbon black and Nafion before (black line) and after chronoamperometry (grey line). The resolution of the peaks is lower than of those shown in Figure 2.1 due to the presence of the FTO electrode and carbon black.

A2 Inductively Coupled Plasma Mass Spectrometry

ICPMS samples were prepared by digesting 150 µg of MOF in 5 mL 67% nitric acid at 120˚C overnight. 144 µL of the resulting solution was added to 9.85 mL of Milli-Q water. The concentration of Zr and Cu ions (in parts per billion) were determined in triplicate. Blank measurements of MilliQ are measured to show the error that can be expected for the measured values. ICPMS measurements for a series of metals were performed on carbon black to exclude any metal impurities.

Table A1. Zr and Cu contents (ppb) of NU1000|Cu-tmpaCOOH and NU1000|$Cu(OTf)_2$ as determined by ICPMS measurements.

Sample ID	Zr 90 (ppb)	Cu 63 (ppb)	Zr : Cu	Catalysts per node	
MilliQ (1% nitric acid)	<0.1	<0.1	-	-	
NU1000|Cu-tmpaCOOH batch 1	89.3	20.0	9 : 2	1.3	
NU1000|Cu-tmpaCOOH batch 1	89.9	21.3	4 : 1	1.5	
NU1000|Cu-tmpaCOOH batch 1	90.4	21.8	4 : 1	1.5	Av = 1.4 (±0.1)[a]
MilliQ (1% nitric acid)	<0.1	<0.1	-	-	
NU1000|Cu-tmpaCOOH batch 1 after CA	19.3	4.3	9: 2	1.3	
NU1000|Cu-tmpaCOOH batch 1 after CA	78.8	14.5	11 : 2	1.1	
NU1000|Cu-tmpaCOOH batch 1 after CA	81.4	15.1	11 : 2	1.1	Av = 1.2 (±0.1) [a]
MilliQ (1% nitric acid)	<0.1	<0.1	-	-	
NU1000|Cu-tmpaCOOH batch 2	106.9	14.2	15 : 2	0.8	
NU1000|Cu-tmpaCOOH batch 2	89.0	11.3	8 : 1	0.8	
NU1000|Cu-tmpaCOOH batch 2	115.4	14.8	8 : 1	0.8	Av = 0.8 (±0.0) [a]
NU1000|$Cu(OTf)_2$	148.2	15.6	19 : 2	1.6	
NU1000|$Cu(OTf)_2$	169.5	19.8	17 : 2	1.4	
NU1000|$Cu(OTf)_2$	185.8	21.0	9 : 1	1.5	Av = 1.5 (±0.1) [a]

[a] average of three measurements with mean deviation to the average in brackets

Table A2. Metal ion contents of carbon black (CB) as determined by ICPMS measurements. The amount of carbon black per sample is equal to the amount of carbon black in 1 dropcast. A value <0.1 means below detection limit.

Sample ID	Zr 90 (ppb)	Cu 63 (ppb)	Co 57 (ppb)	Pd 106 (ppb)	Pt 195 (ppb)	Ni 60 (ppb)	Zn 66 (ppb)	Fe 57 (ppb)
CB	0.1	<0.1	<0.1	<0.1	<0.1	<0.1	<0.1	0.1
CB	0.3	<0.1	<0.1	<0.1	<0.1	<0.1	<0.1	0.0
CB	0.2	<0.1	<0.1	<0.1	<0.1	<0.1	<0.1	0.2

A3 Cyclic Voltammetry

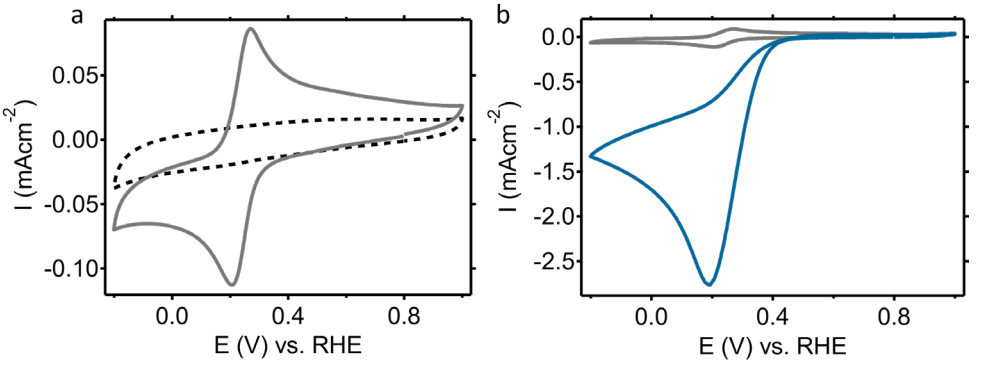

Figure A2. Cyclic voltammograms of a glassy carbon electrode under argon (a, black dotted line), 0.03 mM Cu-tmpaCOOH in 0.1M phosphate buffer pH =7 under argon (a and b, grey line) and Cu-tmpaCOOH under oxygen (b, blue line). Integration of the reduction peak of a shows 3.19 pmol (0.1 nmol cm^{-2}) electrons are transferred.

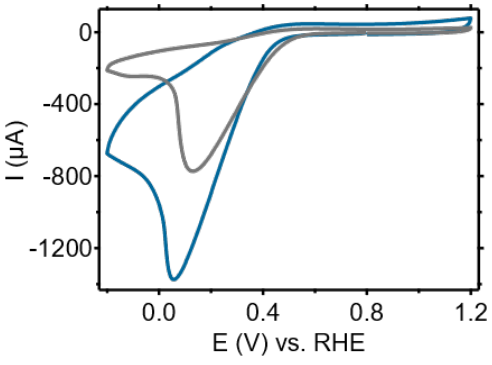

Figure A3. CV of NU1000|Cu-tmpaCOOH batch 1 (blue, 1.4 catalysts per node) and NU1000|Cu-tmpaCOOH batch 2 (grey, 0.8 catalysts per node) in 0.1M phosphate buffer pH =7 at a scan rate of 100 mV s^{-1}.

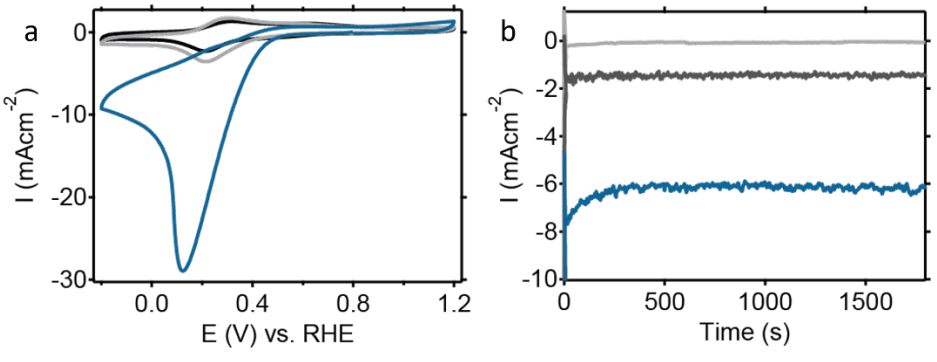

Figure A4. Cyclic Voltammetry (left) and chronoamperometry (right) of NU1000|Cu-tmpaCOOH in 0.1M PB pH = 7. Left: CV was measured under argon (black line), air (light grey line) and 1 atm oxygen (blue line) at 50 mV s^{-1}. Right: CA was measured at 0.3 V vs. RHE under air without stirring (light grey line), under air with stirring (dark grey line) and under oxygen with stirring (blue line). MOF with a loading of 0.8 catalysts per node was used for this experiment.

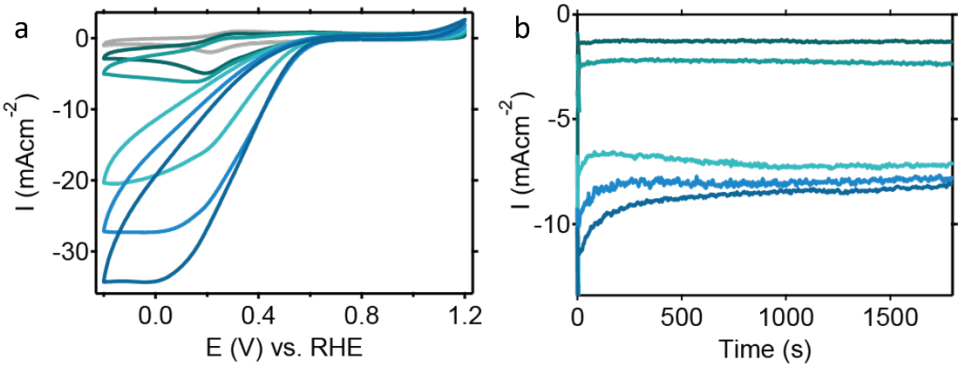

Figure A5. Cyclic Voltammetry at 50 mV s^{-1} (left) and chronoamperometry at 0.3 V vs. RHE (right) of NU1000|Cu-tmpaCOOH in 0.1M PB pH = 7 for a range of H_2O_2 concentrations resulting in increasing current densities: 0 mM, 1.2 mM, 2.4 mM, 10 mM, 15 mM, and 25 mM. CA measurements were performed under constant stirring. MOF with a loading of 0.8 catalysts per node was used for this experiment.

A4 R(R)DE experiments

A.4.1 Koutecky-Levich (K-L) analysis

The electron transfer number (n) was calculated using the (K-L) equation:[1,2]

$$J^{-1} = J_L^{-1} + J_K^{-1} = (B\omega^{1/2})^{-1} + J_K^{-1} \quad (1)$$

$$B = 0.62nFC_{O2}(D_{O2})^{2/3}v^{-1/6} \quad (2)$$

$$J_k = nFkC_{O2} \quad (3)$$

Where J is the measured current density and J_L and J_K are the diffusion and kinetic limiting current, respectively. B is the Levich slope, which is given by equation (2). ω is the rotation rate in rad s^{-1} and is given by $\omega = 2\pi N$, where N is the linear rotation speed. n is the number of electrons transferred per oxygen molecule, C_{O2} is the concentration of O_2 (1.2 mM) and D_{O2} is the diffusion coefficient for O_2 in 0.1 M phosphate buffer (D_{O2}= 1.95E^{-5} cm^2 s^{-1}). v is the kinetic viscosity (v= −0.02 cm^2 s^{-1}) and F is Faraday's constant (F = 96485 C mol^{-1}).

A.4.2 Collection Efficiency of Pt ring

The collection efficiency (N) of the Pt ring for hydrogen peroxide was determined using the 2-electron reduction of O_2 to H_2O_2 by a GC disk. The Pt disk was held at a potential of 1.2 V vs. RHE, as oxidation of H_2O_2 by Pt is mass transport limited at this potential.[3] With a rotation speed of 1600 rpm, CA was measured on the disk by first applying 0.8 V vs. RHE for

60 seconds, followed by −0.1 V vs. RHE for 180 seconds. The ring current (I_r) measured at 0.8 V vs. RHE was used for a background correction of I_r at −0.1 V vs. RHE. Taking Ir over Id for t = 30-60 seconds resulted in a collection efficiency of N = 0.08 (8%).

A.4.3 R(R)DE of Cu-tmpaCOOH in homogeneous solution

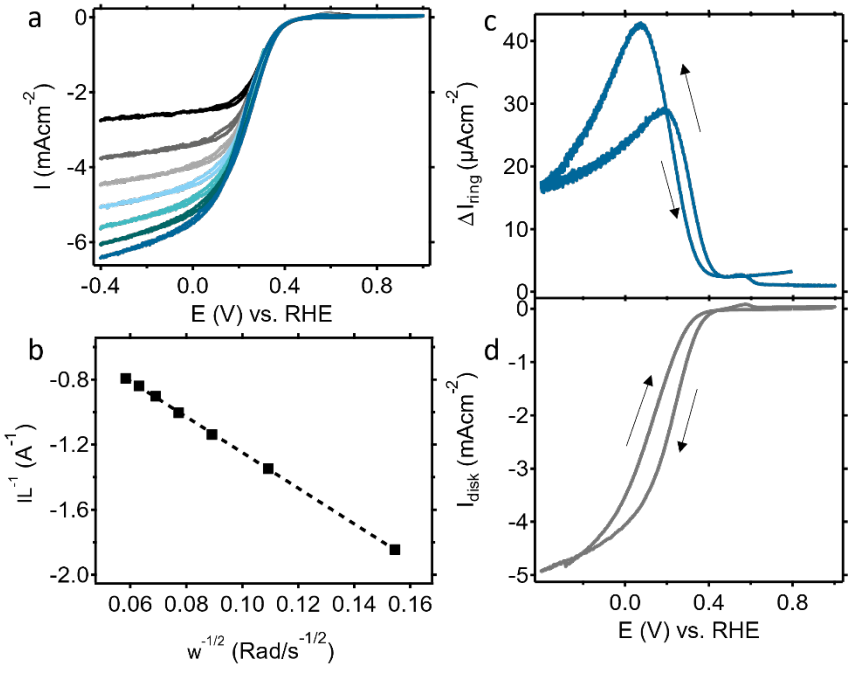

Figure A6. RDE cyclic voltammograms of 0.3 mM Cu-tmpaCOOH in 0.1M PB pH = 7 under oxygen atmosphere at scan rates ranging from 400 rpm (a, black line) to 2800 rpm (a, dark blue line), Koutecky-Levich plot (b) of datapoints at −0.4 V vs. RHE (R^2 = 0.9998) and RRDE cyclic voltammograms at 1600 rpm (c, ring current and d, disk current) at a scan rate of 50 mV s^{-1}.

A5 Vicinity of the catalyst in the pore

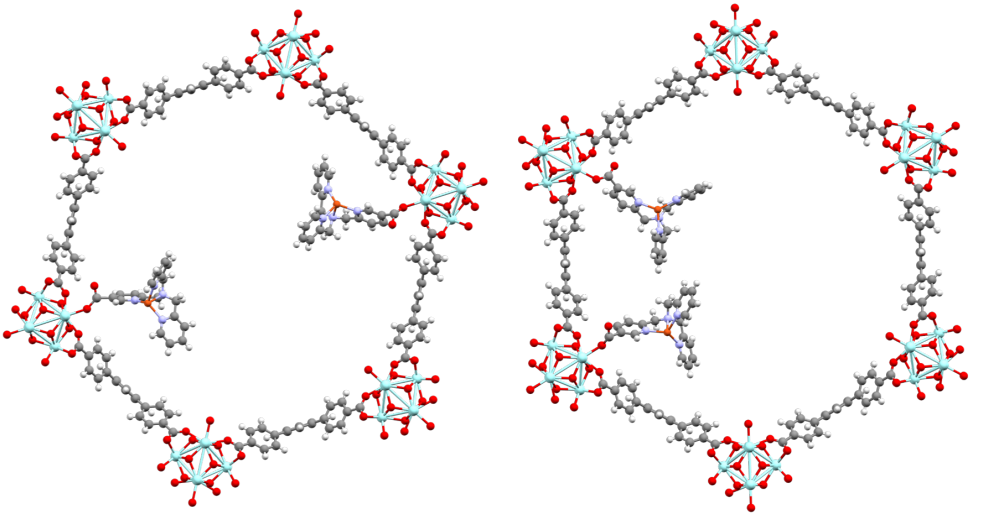

Figure A7. Schematic presentation of a NU1000 pore (31 Å) with two Cu-tmpaCOOH catalysts bound to opposite nodes (left) and adjacent nodes (right). Pore and catalyst structures were adjusted accordingly from CCDC-1580411 and CCDC-2068976 crystal structures respectively. The Cu-Cu distance is approximately 12 Å when the Cu complexes are attached at adjacent nodes and 20 Å when attached to the opposite nodes.

A6 Foot of the Wave Analysis

Foot Of the Wave Analysis (FOWA) was performed on three individual CV measurements for both the oxygen reduction reaction (Figure A8a) and the hydrogen peroxide reduction reaction (Figure A8b) by Cu-tmpaCOOH in homogeneous solution to obtain the TOF_{max} values for this catalyst. In FOWA we consider only the first part of the catalytic wave ($i_c/i_p > 2$) where mass transport limitations do not play a role. The average TOF_{max} of these three measurements is determined as follows:[3,4]

$$\frac{i_c}{i_p} = 2.24n\sqrt{\frac{RT}{Fv}k_{obs}}\, exp\left[-\frac{F}{RT}\left(E - E_{1/2}\right)\right] \quad (4)$$

Where i_c is the peak catalytic current, i_p is the peak current of the one electron reduction of the catalyst, n is the number of electrons used in the catalytic cycle, R is the gas constant, T

is the temperature, F is the faradaic constant, v is the scan rate, k_{obs} is the observed rate constant (k_{obs} = TOF_{max}), E is the potential at the electrode and $E_{1/2}$ is the equilibrium potential of the $Cu^{II/I}$ redox couple. Equation 4 is derived from the FOW analysis of Constantin and coworkers,[4] as was discussed in detail for Cu-tmpa chemistry previously.[3] For both oxygen and hydrogen peroxide reduction, n = 2 since we only look at the beginning of the catalytic wave, where oxygen reduction goes to hydrogen peroxide. TOF_{max} = 3.70 × 10^4 (± 1.05 × 10^4) s^{-1} was found for oxygen reduction and TOF_{max} = 6.75 × 10^4 (± 6.07 × 10^3) s^{-1} for hydrogen peroxide reduction. The catalytic current fits linearly with $1 + exp\,[*RT^{-1}\,(E - E_{1/2})]$, which means the reaction is first order in catalyst, as also reported for Cu-tmpa.

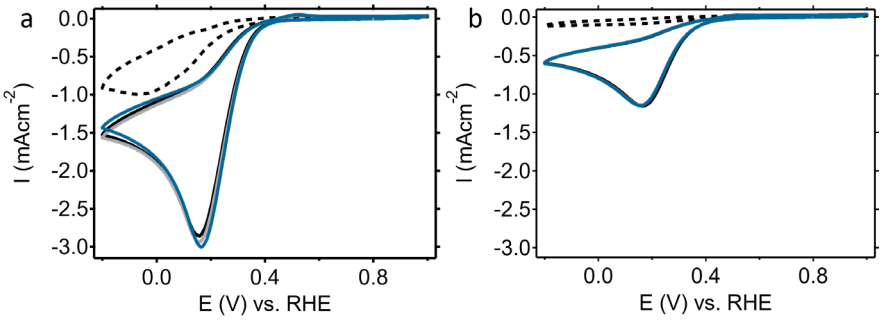

Figure A8. Cyclic Voltammetry of 0.3 mM Cu-tmpaCOOH in 0.1M PB pH = 7 under oxygen atmosphere (a) and under argon atmosphere with 1.2 mM hydrogen peroxide (b) at a scan rate of 100 mV s^{-1}. Blue, grey and black solid lines are triplicate experiments used for FOWA and black dashed lines are glassy carbon blanks.

A

A7 References

[1] J. Li, Y. Chen, Y. Tang, S. Li, H. Dong, K. Li, M. Han, Y. Q. Lan, J. Bao, Z. Dai, *J Mater Chem A Mater* **2014**, *2*, 6316–6319.

[2] W. Yan, Q. Xing, O. Guo, H. Feng, H. Liu, P. Deshlahra, X. Li, Y. Chen, *ACS Appl Mater Interfaces* **2022**, *14*, 50761.

[3] M. Langerman, D. G. H. Hetterscheid, *Angewandte Chemie International Edition* **2019**, *58*, 12974–12978.

[4] C. Costentin, S. Drouet, M. Robert, J. M. Savéant, *J Am Chem Soc* **2012**, *134*, 11235–11242.

Appendix B

Supplementary information for Chapter 3:

Surveying the Homogeneity of a Molecular Electrocatalyst Embedded in a Metal-Organic Framework Using Operando Characterization

B1 Operando XAS cell

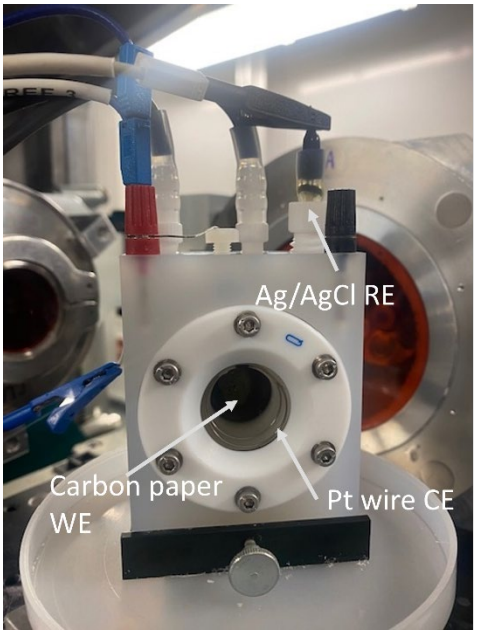

Figure B1 Electrochemical cell used for operando X-ray absorption measurements.

B2 XANES

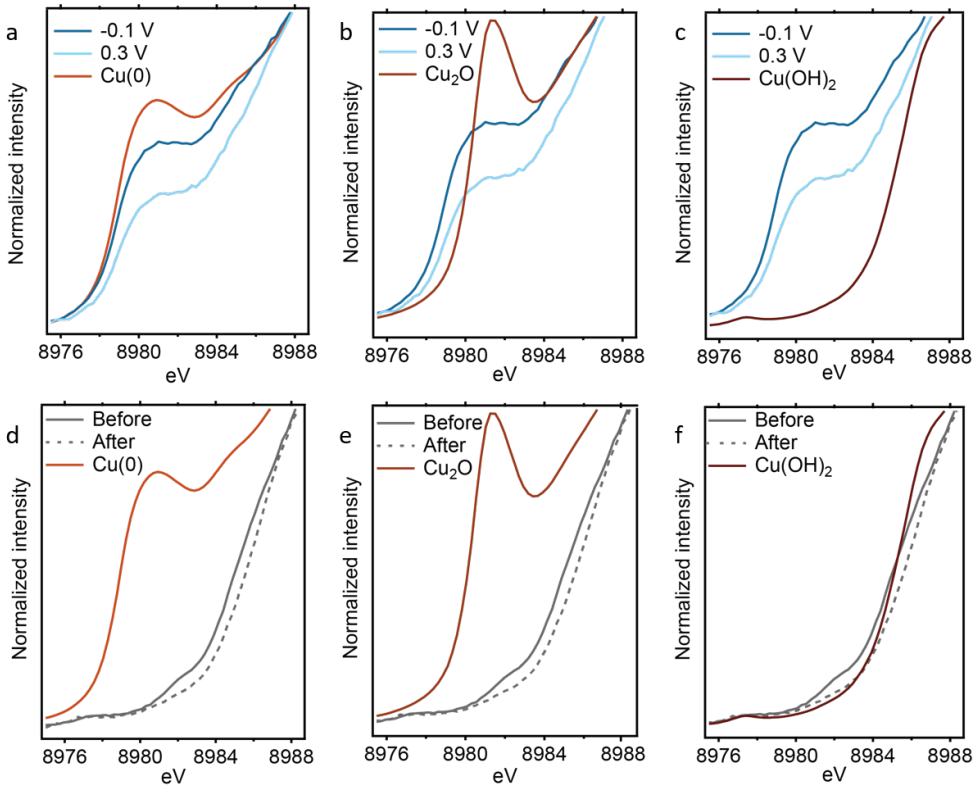

Figure B2 Pre-edge region of Cu K-edge XANES spectra of NU1000|Cu-tmpaCOOH under O_2 atmosphere at 0.3 V vs. RHE applied potential (light blue), −0.1 V vs. RHE applied potential (dark blue) before (grey) and after (grey dashed) applying a potential as well as pre-edge region of XANES spectra of Cu references.

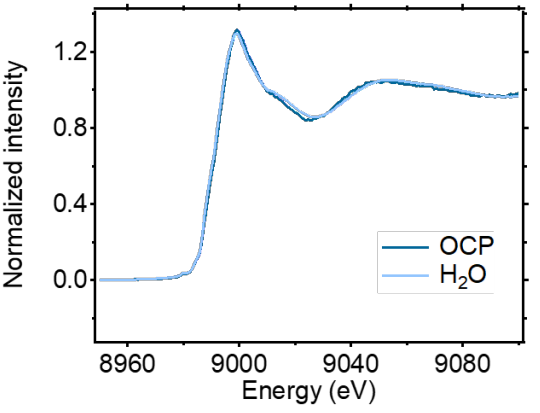

Figure B3 Cu K-edge XANES spectra of NU1000|Cu-tmpaCOOH in H_2O and in O_2 saturated phosphate buffer pH 7 at OCP.

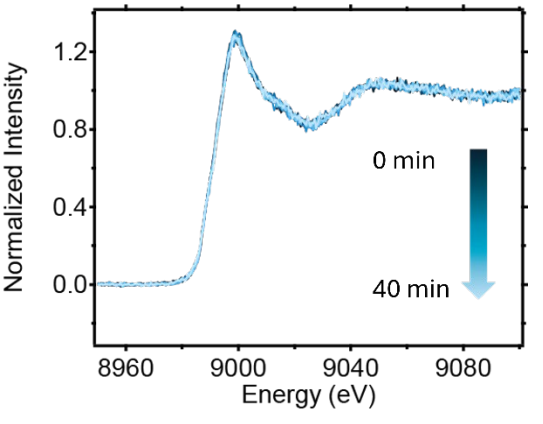

Figure B4 Cu K-edge XANES spectra of NU1000|Cu-tmpaCOOH in O_2 saturated phosphate buffer pH 7 at OCP subsequently measured, 9 scans, 5-minute long each for a total of 40 minutes.

Table B1. Fractions of Cu oxidation states found at −0.1 V and 0.3 V vs. RHE as determined from LCF in Figure 3.2.

NU1000|Cutmpa-COOH O_2	**Cu(0)**	**$Cu(I)_2O$**	**$Cu(II)(OH)_2$**	**R-factor**	**χ^2**
−100 mV (vs. RHE)	0.776		0.224	0.006	0.238
	0.60	0.40		0.010	0.256
300 mV (vs. RHE)	0.487		0.513	0.013	0.587
	0.24	0.76		0.039	1.218

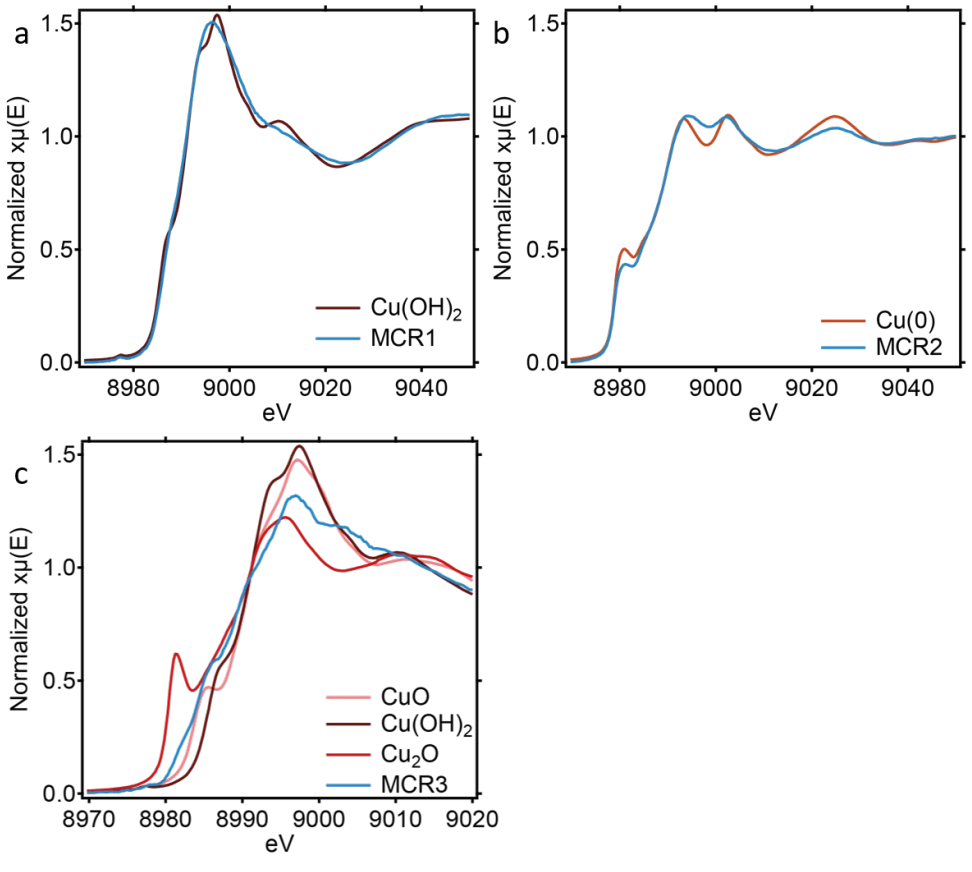

Figure B5 Comparison of the Cu K-edge XANES of the different MCR fitting elements identified for the NU1000|Cu-tmpaCOOH in O_2 saturated phosphate buffer pH 7 at −0.1 V vs. RHE with Cu standards. (a) MCR1 compared to $Cu(OH)_2$, (b) MCR2 to Cu^0 foil, and (c) MCR3 to CuO, Cu_2O and $Cu(OH)_2$.

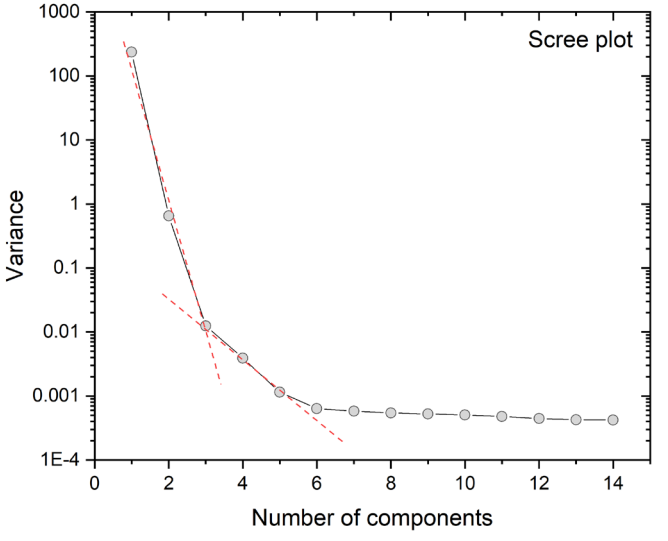

Figure B6 Variance of the Cu K-edge operando data set as a function of the number of components. The obtained MCR components were compared with standards of known oxidation state (Figure B5). The 1st MCR component overlaps with $Cu(OH)_2$, representing Cu^{2+}. The 2nd MCR component represents metallic Cu^0 nanoparticles. The 3rd MCR component has similar features to the CuO spectrum, but does not fully overlap.

B3 Electrochemistry for operando XAS

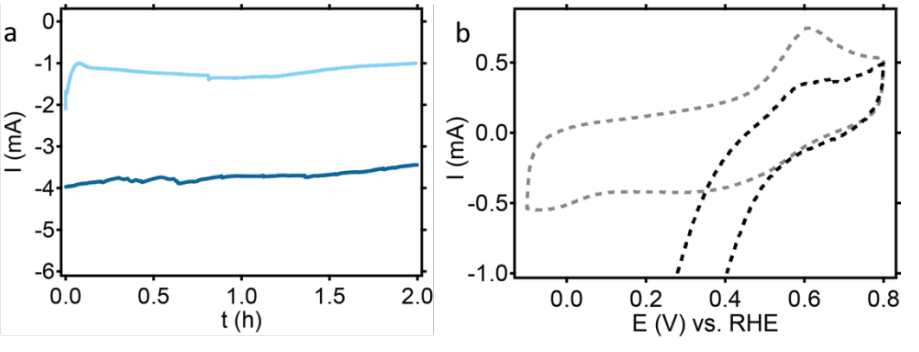

Figure B7 CA of NU1000|Cu-tmpaCOOH under O_2 atmosphere at 0.3 V vs. RHE (a, light blue) and −0.1 V vs. RHE (a, dark blue) measured during operando XANES and EXAFS shown in Figure 3.2 and Figure 3.4 CV under He atmosphere after CA under O_2 atmosphere (b, black dashed) and after CA under He atmosphere (b, grey dashed).

Appendix C

Supplementary information for Chapter 4:

The Effect of a Redox-Active Metal-Organic Framework on the Catalyst Activity and Stability

C1 Inductively Coupled Plasma Mass Spectrometry

ICPMS samples were prepared by digesting 150 µg of MOF in 5 mL 67% nitric acid at 120˚C overnight. 144 µL of the resulting solution was added to 9.85 mL of Milli-Q water. The concentration of Zr and Cu or Co ions (in parts per billion) were determined in triplicate. Blank measurements of MilliQ are measured to show the error that can be expected for the measured values.

Table C1 Zr and Cu contents (ppb) of Zr-(BTD-NDI)|Cu-tmpaCOOH as determined by ICPMS measurements.

Sample ID	Zr 90 (ppb)	Cu 63 (ppb)	Zr : Cu	Catalysts per node	
MilliQ (1% nitric acid)	<0.1	<0.1	-	-	
Zr-(BTD-NDI)|Cu-tmpaCOOH batch 1	67.184	15.354	9: 2	1.37	
Zr-(BTD-NDI)|Cu-tmpaCOOH batch 1	73.237	13.734	11 : 2	1.13	
Zr-(BTD-NDI)|Cu-tmpaCOOH batch 1	69.013	10.309	7 : 1	0.90	Av = 1.13 (±0.13) [a]
MilliQ (1% nitric acid)	<0.1	<0.1	-	-	
Zr-(BTD-NDI)|Cu-tmpaCOOH batch 2	46.241	4.911	9 : 1	0.64	
Zr-(BTD-NDI)|Cu-tmpaCOOH batch 2	60.021	6.844	9 : 1	0.68	
Zr-(BTD-NDI)|Cu-tmpaCOOH batch 2	61.400	6.724	9 : 1	0.66	Av = 0.66 (±0.01) [a]
MilliQ (1% nitric acid)	<0.1	<0.1	-	-	
Zr-(BTD-NDI)|$Cu(OTf)_2$	60.424	60.217		5.98	

Zr-(BTD-NDI)|$Cu(OTf)_2$	64.463	61.766		5.75	
Zr-(BTD-NDI)|$Cu(OTf)_2$	63.070	57.128		5.43	Av = 5.72 (±0.19) [a]

[a] average of three measurements with the mean deviation from the average between brackets

Table C2 Zr and Co contents (ppb) of Zr-(BTD-NDI)|CoCp(CpCOOH) and NU1000|CoCp(CpCOOH) as determined by ICPMS measurements.

Sample ID	**Zr 90 (ppb)**	**Co 59 (ppb)**	**Zr : Co**	**Catalysts per node**	
Zr-(BTD-NDI)| CoCp(CpCOOH)	28.9	16.5	7 : 4	3.3	
Zr-(BTD-NDI)| CoCp(CpCOOH)	21.5	12.0	7 : 4	3.4	
Zr-(BTD-NDI)|Co Cp(CpCOOH)	14.6	8.6	17 : 10	3.6	Av = 3.4 (±0.01) [a]
NU1000|Co Cp(CpCOOH)	45.4	11.9	4 : 1	1.6	
NU1000|Co Cp(CpCOOH)	41.8	10.9	4 : 1	1.6	
NU1000|Co Cp(CpCOOH)	35.1	9.2	4 : 1	1.6	Av = 1.6 (±0.01) [a]

[a] average of three measurements with the mean deviation from the average between brackets

C2 Electrochemistry

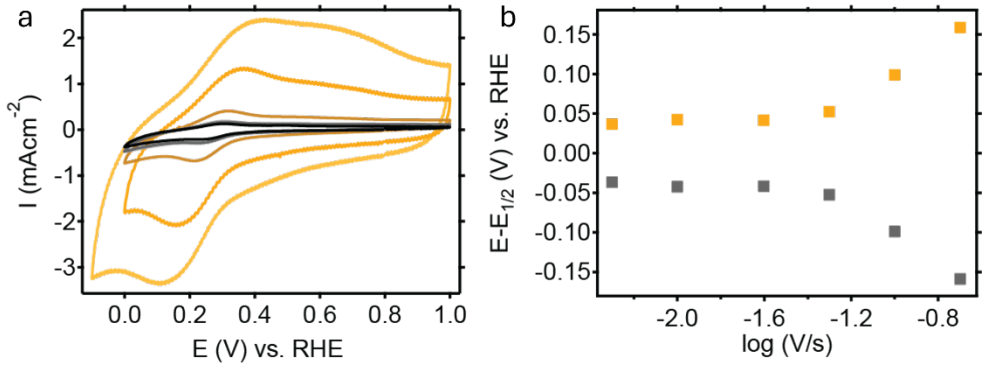

Figure C1 Cyclic voltammograms under argon of Zr-(BTD-NDI)|Cu-tmpaCOOH at scan rates ranging from 5 mV s^{-1} (a, black) to 200 mV s^{-1} (a, light yellow) in 0.1 M phosphate buffer pH 7, and corresponding Laviron plot for the $Cu^{II/I}$ redox couple (b).

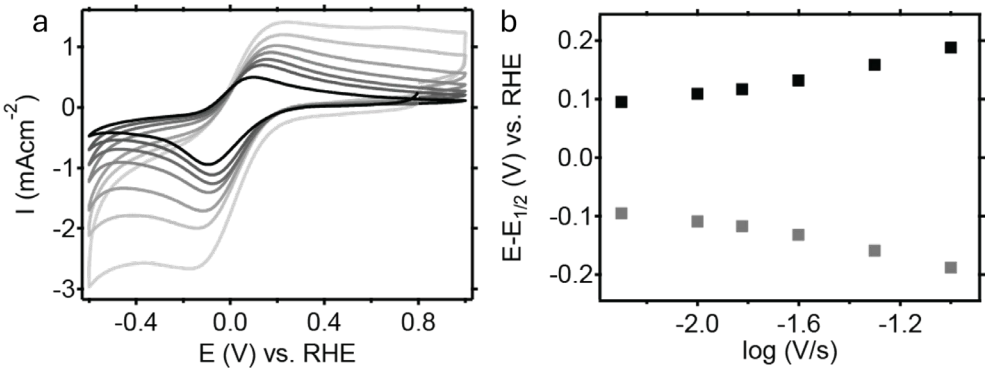

Figure C2 Cyclic voltammograms under argon of Zr-(BTD-NDI) at scan rates ranging from 5 mV s^{-1} (a, black) to 200 mV s^{-1} (a, light grey) in 0.1 M phosphate buffer pH 7, and corresponding Laviron plot for the NDI/NDI^{2-} 2-electron transfer (b).

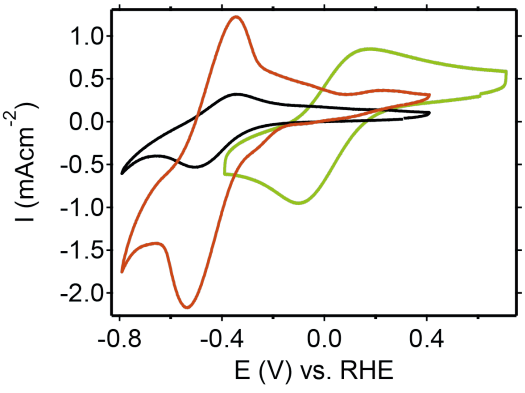

Figure C3 Cyclic voltammograms of Zr-(BTD-NDI) (green), Zr-(BTD-NDI)|CoCp(CpCOOH) (red) and NU1000|Co Cp(CpCOOH) (black) under argon atmosphere at a scan rate of 50 mVs^{-1}.

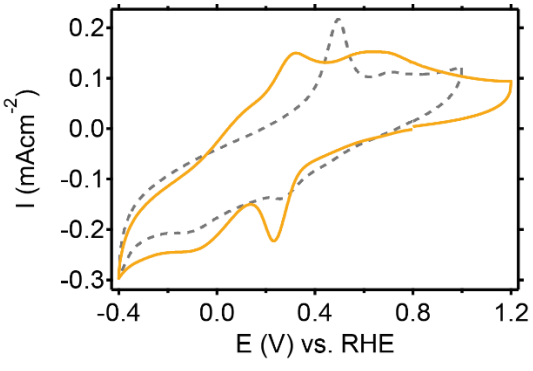

Figure C4 Cyclic voltammograms with a scan rate of 50 mVs^{-1} of Zr-(BTD-NDI)|Cu-tmpaCOOH under argon atmosphere before (yellow) and after (grey intermittent) ORR at −0.1 V vs. RHE.

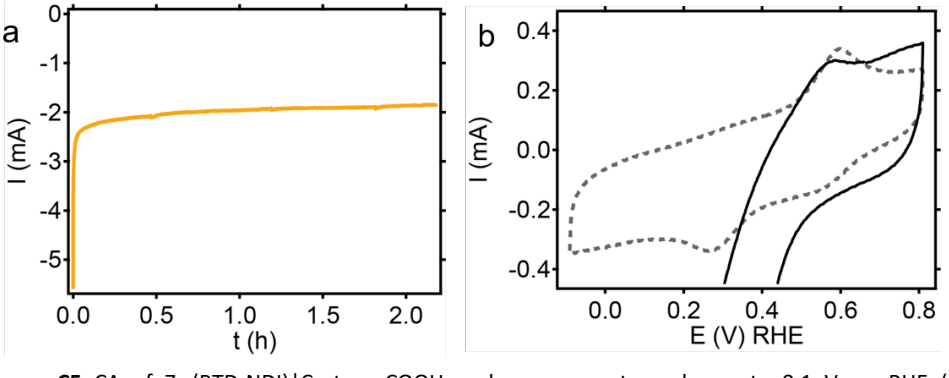

Figure C5 CA of Zr-(BTD-NDI)|Cu-tmpaCOOH under oxygen atmosphere at −0.1 V vs. RHE (a) corresponding to operando XANES and EXAFS shown in Figure 4.7, 4.8 and 4.9 and CV under helium atmosphere after CA under oxygen atmosphere (b, black) and after CA under helium atmosphere (b, grey intermittent).

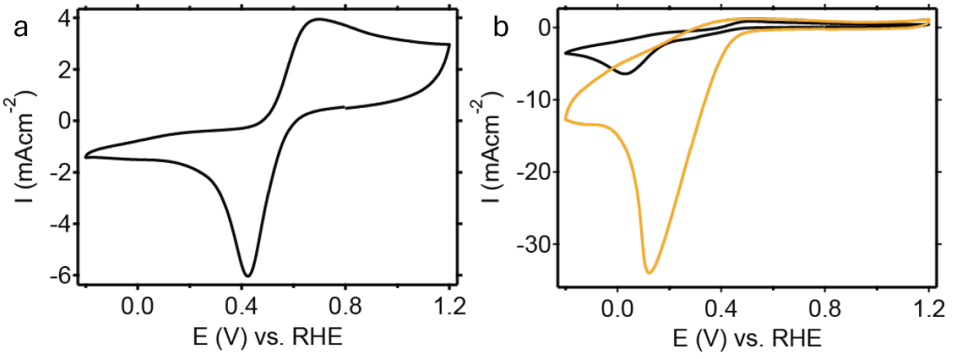

Figure C6 CV of Zr-(BTD-NDI)|$Cu(OTf)_2$ under argon (a) and CV of Zr-(BTD-NDI)|$Cu(OTf)_2$ (black) and of Zr-(BTD-NDI)|Cu-tmpaCOOH (yellow) under oxygen atmosphere (b).

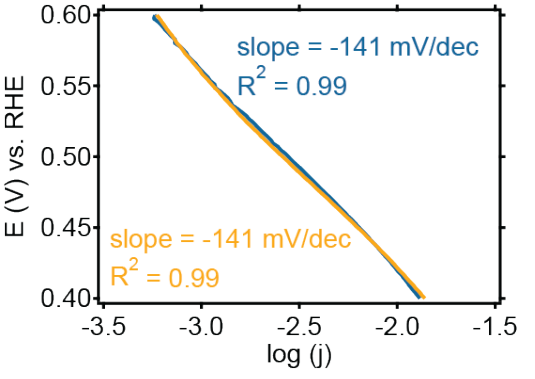

Figure C7 Tafel plot for the ORR catalyzed by Zr-(BTD-NDI)|Cu-tmpaCOOH (yellow) and NU1000|Cu-tmpaCOOH (blue), corresponding to figure 4.11. The Tafel slopes are given in mV/dec.

C

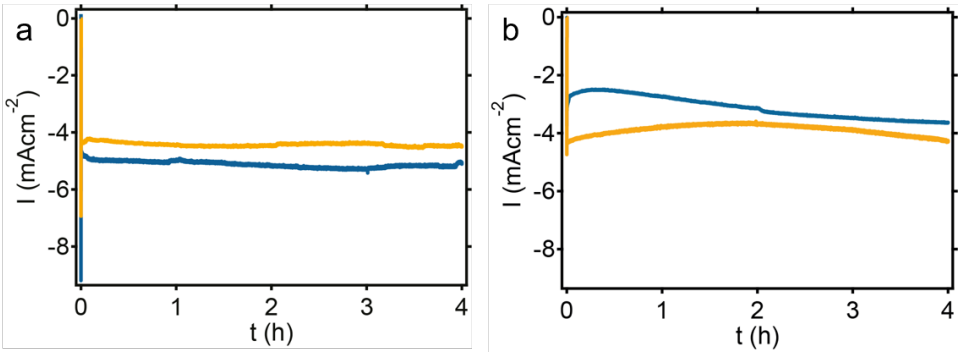

Figure C8 Chronoamperometry at −0.1 V vs. RHE under oxygen atmosphere of Zr-(BTD-NDI)|Cu-tmpaCOOH (yellow) and NU1000|Cu-tmpaCOOH (blue).

C3 Electron Transfer Efficiency calculations

Chronoamperometry (CA) under Ar atmosphere at −0.49 V vs. RHE was measured until the charge stabilizes. The % of redox active moieties reduced is determined according to the following equation:

$$\%\ of\ redox\ active\ moieties\ reduced\ = \frac{n}{n_T} \times\ 100 \quad \text{(C1)}$$

Where n is the number of electrons transferred and n_T is the theoretical maximum number of electrons transferred.
n can be calculated from the measured charge as follows:

$$n\ = \frac{6.25E18 \times Q}{N_A} \quad \text{(C2)}$$

Where Q is the measured charge in coulombs and N_A is Avogadro's number.

n_T can be calculated from the total number of redox active moieties in the MOF, which in turn can be determined from the mass of MOF in the dropcast, the molar mass of the MOF and the loading of the catalyst in the MOF (Equation C3). For this calculation, it should be considered that the $Co^{III/II}$ transition is a one-electron transition and the NDI/NDI^{2-} transition is a two-electron transition. Each MOF unit cell contains two linkers and one node and the molar mass of a unit cell NU1000 is 2177 g/mol and the molar mass of a unit cell Zr-(BTD-NDI) is 2609 g/mol. For these experiments, a 10 µL dropcast containing 100 µg MOF was used.

$$n_T = (\ mol\ NDI\ linkers\ \times 2\ )\ + mol\ CoCp(CpCOOH) \quad \text{(C3)}$$

For Zr-(BTD-NDI) this means 100 µg with a molar mass of 2609 µg/µmol per unit cell, which equals to 0.0383 µmol Zr-(BTD-NDI), was dropcasted on the electrode. Therefore, there were 38.3 nmol unit cells that each have two linkers, which equals to 76.6 nmol linkers. Two electrons per linkers results in a total n_T of 153.2 nmol electrons.

For Zr-(BTD-NDI)|CoCp(CpCOOH), there are the same number of linkers, equating to 153.2 electrons as well. The MOF has a CoCp(CpCOOH) loading of 3.4 Co per node. With 38.3 unit cells, that each contain 1 node, this loading results in a total Co content of 130.22 nmol. The n_T for this MOF therefore equals 153.2 + 130.22 = 283.42 nmol electrons.

For NU1000|CoCp(COOH) we have 100 µg with a molar mass of 2177 µg/µmol per unit cell, which equals 0.046 µmol unit cells dropcasted onto the electrode. As one unit cell contains 1 node, we have 46 nmol nodes. With a loading of 1.57 Co per node, this equals to 72.22 nmol Co. As Co is the only redox active moiety in this MOF, and a single electron can be transferred per Co center, the n_T for this MOF equals 72.22 nmol electrons.

Table C3 Values calculated to determine the % of redox active moieties activated during CA under Ar atmosphere for Zr-(BTD-NDI), NU1000|CoCp(CpCOOH) and Zr-(BTD-NDI)|CoCp(CpCOOH).

MOF	n_T (nmol)	n (nmol)	Q (mC)	% of redox active moieties reduced
Zr-(BTD-NDI)	153	1.89	0.182	1
NU1000|CoCp(CpCOOH)	72	2.17	0.209	3
Zr-(BTD-NDI) |CoCp(CpCOOH)	283	70	6.74	25

C4 Electrochemical Impedance Spectroscopy

Electrochemical impedance spectroscopy (EIS) was measured for Zr-(BTD-NDI)|CoCp(CpCOOH) (orange), Zr-(BTD-NDI) (green) and NU1000|CoCp(CpCOOH) to estimate the resistance experienced by electrons propagating through these MOFs. EIS was measured at potentials of 0.41, 0.01 and −0.49 V vs. RHE at frequencies between 0.1 MHz and 0.1 Hz at an amplitude of 0.01 V. It is important to note that the Ohmic resistance shown in these Nyquist plots is the combined resistance of a system that contains multiple interfaces. The electrode-MOF interface, MOF-electrolyte interface, grain boundaries and pores make fitting and interpreting of the data to an appropriate circuit difficult. Therefore, the absolute values obtained here may not be directly correlated to the resistance within the MOF. We can however observe a trend in Ohmic resistance, that is in good agreement

with the results obtained for the electron transfer efficiencies in these MOFs: the lower the Ohmic resistance, the more redox active moieties can be addressed.

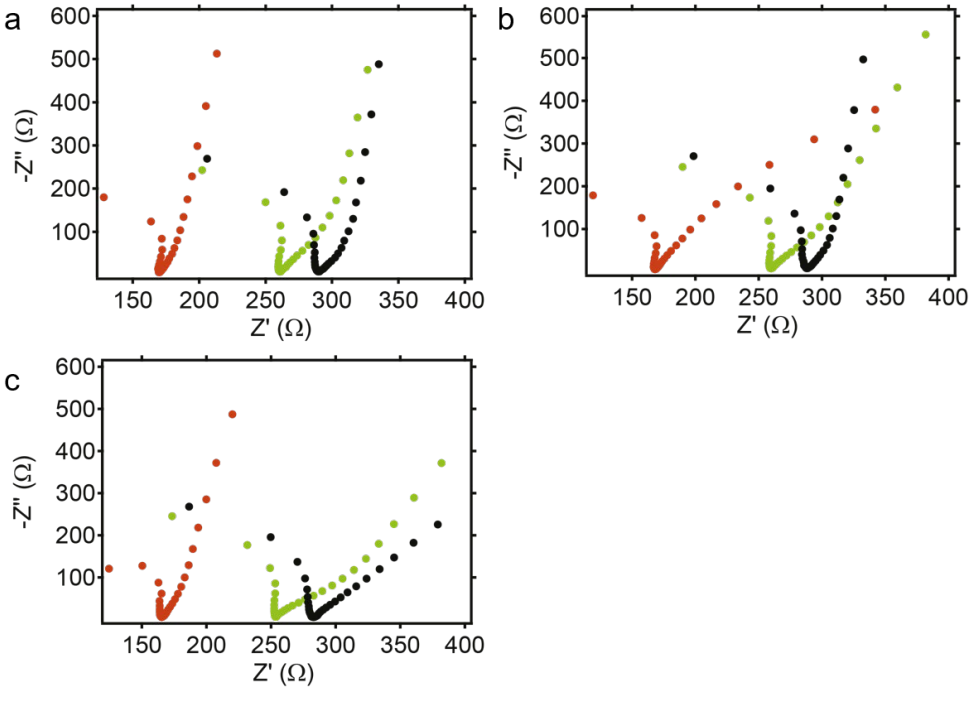

Figure C9 Nyquist plots for Zr-(BTD-NDI)|CoCp(CpCOOH) (orange), Zr-(BTD-NDI) (green) and NU1000|Co Cp(CpCOOH) (black) measured at 0.41 V vs. RHE (a), 0.01 V vs. RHE (b) and −0.49 V vs. RHE (c).

C5 X-ray Absorption Spectroscopy

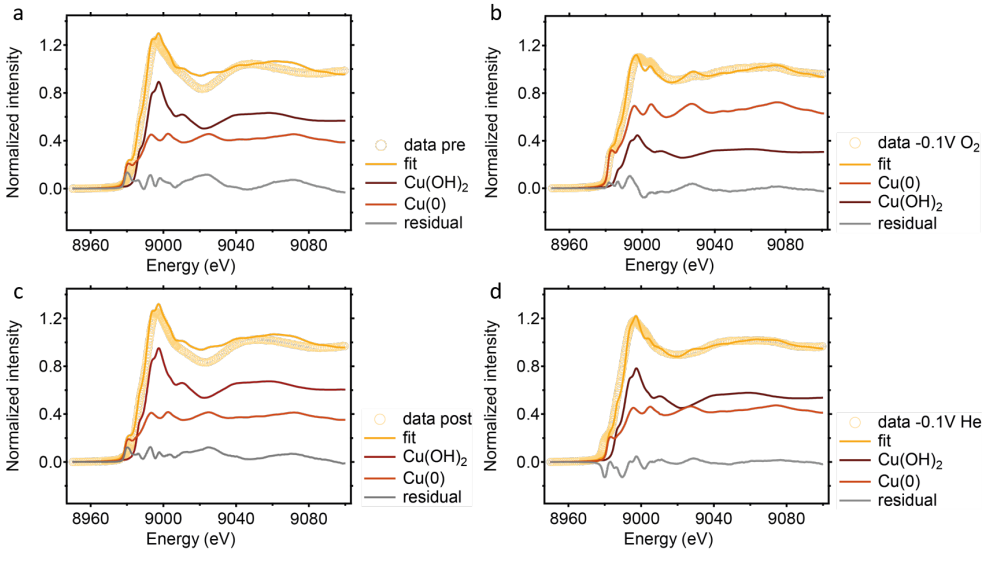

Figure C10 Linear combination fitting (LCF) of the XANES spectrum of Zr-(BTD-NDI)|Cu-tmpaCOOH at OCP (a), at −0.1 V vs. RHE under O_2 atmosphere (b), at OCP after ORR (c) and at −0.1 V vs. RHE under He atmosphere (d) with $Cu(OH)_2$ and Cu(0).

Table C4 Fractions of Cu oxidation states found at −0.1 V vs. RHE and OCP under O_2 or He atmosphere as determined from LCF in Figure C10.

Zr-(BTD-NDI)|Cu-tmpaCOOH	Cu-foil	$Cu(OH)_2$	R-factor	Chi-square
OCP pre, O_2	0.420	0.580	0.016	0.646
−0.1 V vs. RHE, O_2	0.686	0.314	0.012	0.332
OCP post, O_2	0.381	0.619	0.022	0.753
−0.1V vs. RHE, He	0.449	0.551	0.014	0.454

Appendix D

Supplementary information for Chapter 5:

The Effect of pH on Charge Transport in a Naphthalene Diimide Metal-Organic Framework in Aqueous Electrolyte

D1 Cyclic Voltammetry

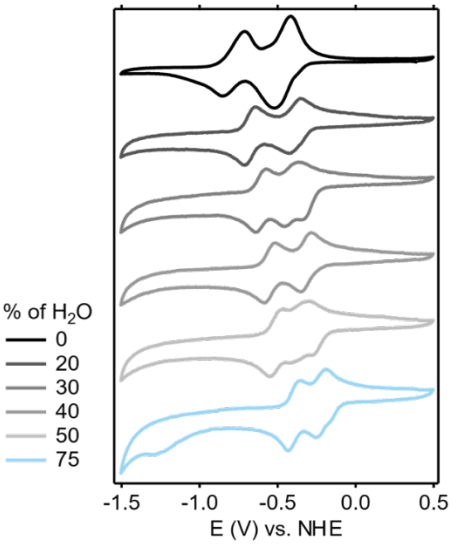

Figure D1 CV of 1 mM dcphOH-NDI in 0.1 KPF_6 in DMF with increasing percentage of water.

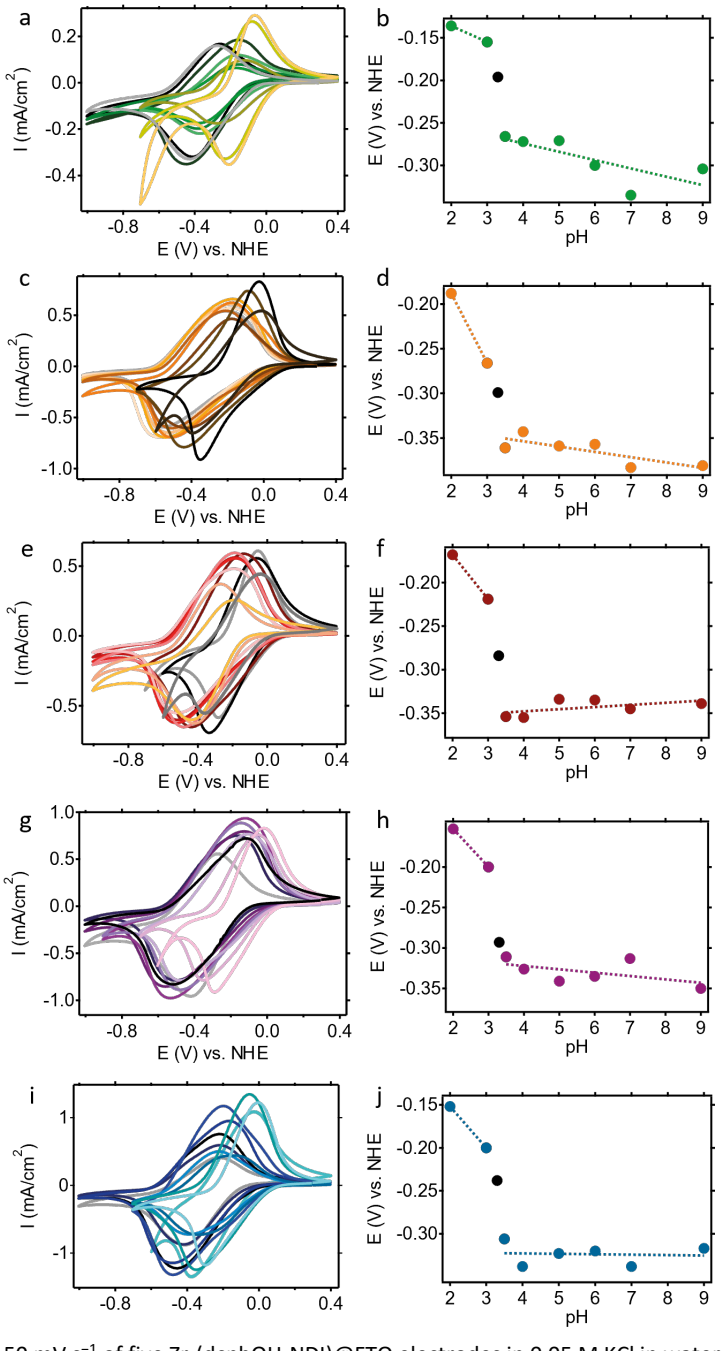

Figure D2 CV at 50 mV s^{-1} of five Zr-(dcphOH-NDI)@FTO electrodes in 0.05 M KCl in water at pH 2 – 9 (left panels) and corresponding Pourbaix diagrams (right panels). pH of the electrolyte was adjusted to HCl and KOH.

D2 Ohmic Resistance

The Ohmic resistance of Zr-(dcphOH-NDI)@FTO was determined at pH 2–4 following a literature procedure.[1] Two potential steps (0 V and 0.5 V vs. NHE) in the double layer region of CV were applied for a duration of 16 ms. The rate by which the current changes, determined by the slope between two points on the time vs. current plot directly after stepping the potential, is inversely proportional to the resistance. The uncompensated resistance R (Ω) is calculated following Ohm's law:

$$R = \frac{\Delta E}{i_0}$$

Where ΔE is the difference between the two potentials chosen and i_0 the initial current.

Table D1 Ohmic resistance of Zr-(dcphOH-NDI)@FTO at pH 2−4.

pH	R (Ω)
2	1.1×10^5
3	1.4×10^5
3.5	1.0×10^5
4	1.1×10^5

D3 Apparent Diffusion Coefficient

The influence of pH on the speed of electron transfer through the framework was evaluated by determining the apparent diffusion coefficient (D_e^{app}) of electron hopping. D_e^{app} values were determined by Equations D1 and D2 as previously reported.[2]

$$\Gamma e = \frac{|Q|}{nFS_A} \quad \text{(D1)}$$

$$D_e^{app} = \left(\frac{slope\ x\ df\ \sqrt{\pi}}{nF\Gamma e}\right)^2 \quad \text{(D2)}$$

Γe is the concentration of electro-active linkers (mol/cm^2), Q is charge in coulomb, n is the number of electrons transferred, F is the Faraday constant, S_A is the surface area of the MOF

film (cm^2), slope is the slope of the Cottrell plot (A $s^{1/2}$ cm^{-2}), and d_f is the film thickness (cm). These parameters are determined from charge and current plots, Cottrell plots and SEM pictures to determine the film thickness, as shown in Figure D3. Table D2 shows the values for the parameters for a pH range from pH 2 to pH 7. The Cottrell plot is described by the Cottrell equation (Equation D3).

$$j\,(t) = \frac{nFS_A\Gamma_e\sqrt{D_e^{app}}}{\sqrt{\pi}\sqrt{t}} \qquad \text{(D3)}$$

Where n is the number of electrons transferred, F is the Faraday's constant, S_A is the electrode surface area, Γe is the concentration of electroactive species and D_e^{app} is the diffusion constant for these electroactive species.

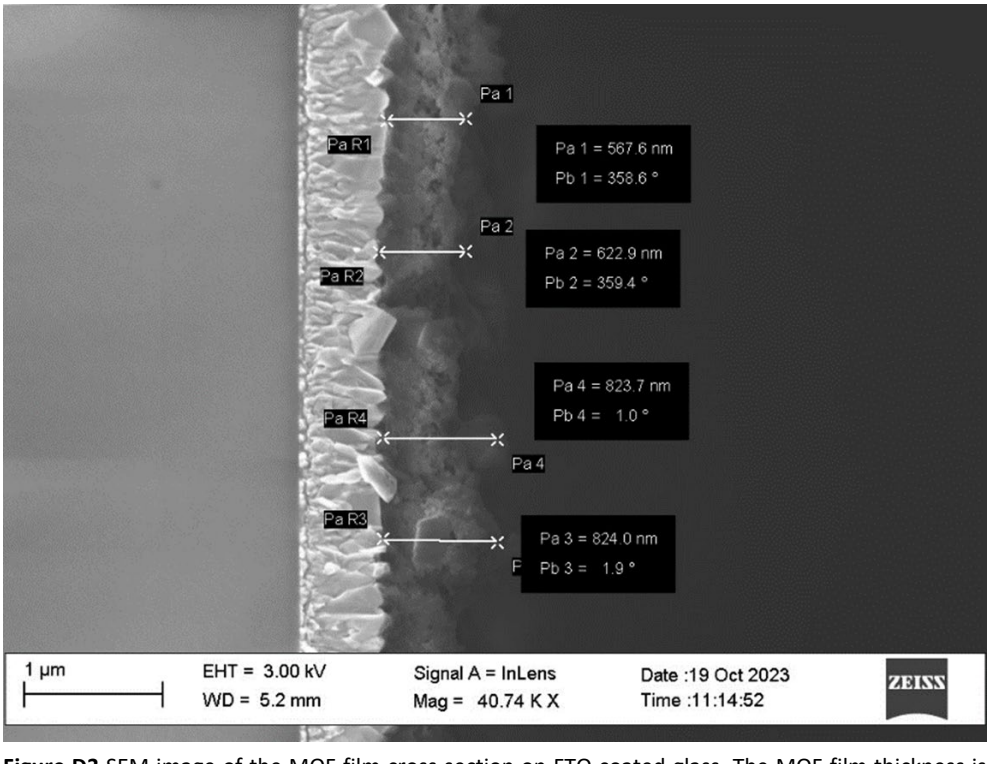

Figure D3 SEM image of the MOF film cross section on FTO coated glass. The MOF film thickness is indicated at four places.

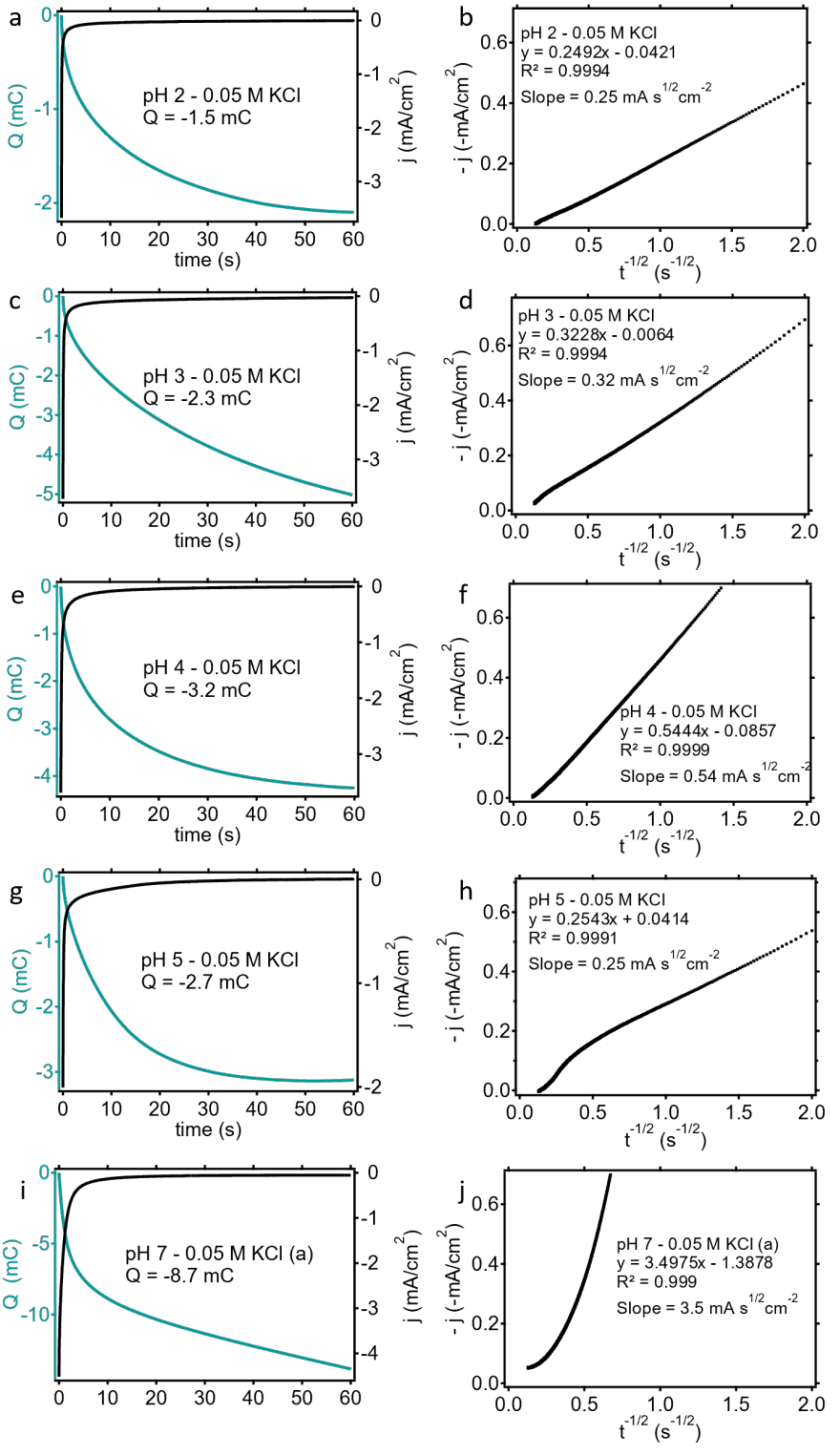
a
pH 2 - 0.05 M KCl
Q = -1.5 mC
Q (mC)
j (mA/cm²)
time (s)
b
pH 2 - 0.05 M KCl
y = 0.2492x - 0.0421
R² = 0.9994
Slope = 0.25 mA s^1/2cm^-2
- j (-mA/cm²)
t^-1/2 (s^-1/2)
c
pH 3 - 0.05 M KCl
Q = -2.3 mC
d
pH 3 - 0.05 M KCl
y = 0.3228x - 0.0064
R² = 0.9994
Slope = 0.32 mA s^1/2cm^-2
e
pH 4 - 0.05 M KCl
Q = -3.2 mC
f
pH 4 - 0.05 M KCl
y = 0.5444x - 0.0857
R² = 0.9999
Slope = 0.54 mA s^1/2cm^-2
g
pH 5 - 0.05 M KCl
Q = -2.7 mC
h
pH 5 - 0.05 M KCl
y = 0.2543x + 0.0414
R² = 0.9991
Slope = 0.25 mA s^1/2cm^-2
i
pH 7 - 0.05 M KCl (a)
Q = -8.7 mC
j
pH 7 - 0.05 M KCl (a)
y = 3.4975x - 1.3878
R² = 0.999
Slope = 3.5 mA s^1/2cm^-2

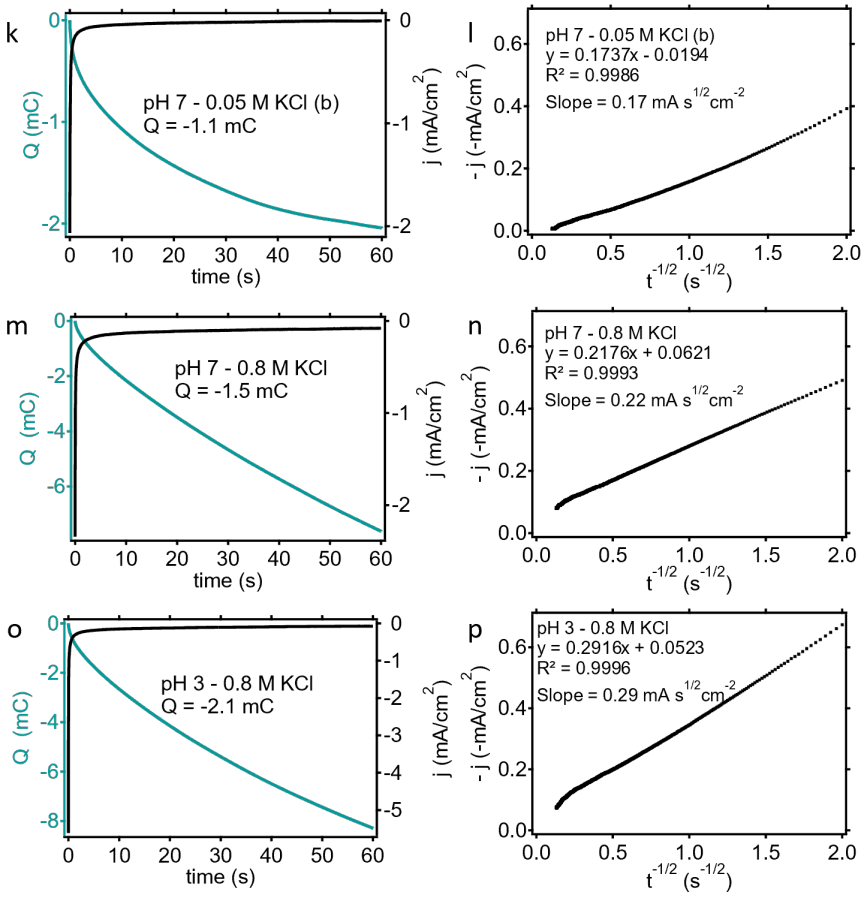

Figure D4 Charge vs. time and current vs. time plots (left) and Cottrell plots (right) for Zr-(dcphOH-NDI)@FTO in 0.05 M KCl or 0.8 M KCl at varying pH. The potentials applied during CA measurements can be found in Table D2.

Table D2 Apparent diffusion coefficients for Zr-(dcphOH-NDI)@FTO thin films at pH 2–7.

E (V vs. AgAgCl)	[KCl] M	pH	S_A (cm^2)	d_f (μm)	Q (m)	Cottrell slope	Γe ($mol*cm^{-2}$)	D_e^{app} (cm^2s^{-1})
−0.7	0.05	2	1.1	0.51	−1.5	0.25	7.07×0^{-9}	2.75×10^{-10}
−0.7	0.05	3	1.1	0.81	−2.3	0.32	1.65×10^{-8}	4.83×10^{-10}
−0.75	0.05	4	1.3	0.72	−3.2	0.54	1.28×10^{-8}	7.84×10^{-10}
−0.75	0.05	5	1.5	0.66	−2.7	0.25	9.33×10^{-9}	2.64×10^{-10}
−0.8	0.05	7	1.1	0.97	−8.7	3.5	4.1×10^{-8}	5.79×10^{-9}
−0.7	0.05	7	0.9	0.82	−1.1	0.17	6.33×10^{-9}	4.11×10^{-10}
−0.7	0.8	7	0.7	0.67	−1.5	0.22	1.11×10^{-8}	1.46×10^{-10}
−0.7	0.8	3	0.8	0.71	−2.1	0.29	1.36×10^{-8}	1.93×10^{-10}

D4 References

[1] N. Elgrishi, K. J. Rountree, B. D. McCarthy, E. S. Rountree, T. T. Eisenhart, J. L. Dempsey, *J Chem Educ* **2018**, *95*, 197–206.

[2] A. T. Castner, H. Su, E. Svensson Grape, A. K. Inge, B. A. Johnson, M. S. G. Ahlquist, S. Ott, *J Am Chem Soc* **2022**, *144*, 5910–5920.